PURPOSE-LED
PUBLISHING™

PAPER • OPEN ACCESS

Identification of synthetic parameters for the thermal characterization of Phase Change Materials in MH-PCM hydrogen storage systems

To cite this article: V. K. Krastev *et al* 2024 *J. Phys.: Conf. Ser.* **2893** 012071

View the article online for updates and enhancements.

Identification of synthetic parameters for the thermal characterization of Phase Change Materials in MH-PCM hydrogen storage systems

V. K. Krastev[1]*, M. Baldelli[2], L. Bartolucci[2], S. Cordiner[2], G. Falcucci[1] and V. Mulone[2]

[1] Enterprise Engineering Dept., University of Rome "Tor Vergata", Rome, Italy
[2] Industrial Engineering Dept., University of Rome "Tor Vergata", Rome, Italy

*E-mail: krastev@dii.uniroma2.it

Abstract. The present work adopts a multidimensional CFD methodology to investigate the thermal coupling between Phase Change Materials coupled and intermetallic Metal Hydrides, for hydrogen storage and delivery. In contrast to the currently available literature on this topic, the focus here is shifted from specific application-oriented modeling towards the systematic identification of a minimum set of parameters to highlight eventual similarity patterns among different PCM families. To achieve this goal, a representative cylindrical-type MH-PCM system model has been defined for a discharge-mode configuration, taking into account engineering-related constraints like the optimal hydrogen pressure delivery and hydrogen massflow control. The results obtained are expected to significantly improve design practices based on standard CFD methods, as well as to pave the way for the derivation of fast and accurate data-driven model surrogates for real-time modeling applications.

1. Introduction

Following the path already set by EU's Hydrogen Strategy [1], in its current 2024 implementation [2] the Clean Hydrogen JU Work Programme covers research and innovation activities grouped into three strategic pillars: I) Renewable Hydrogen Production; II) Hydrogen storage and distribution; III) Hydrogen end uses (transport and clean heat/power applications). Regarding hydrogen storage, specific research targets are identified in terms of safety, energy efficiency, environmental compatibility and cost competitiveness compared to the currently available state-of-the-art compressed hydrogen technology.

Metal Hydrides (MH) are promising solid-state hydrogen carriers, due to their moderate operating pressure and temperature, as well as their potentially disruptive volumetric storage density compared to standard compressed hydrogen storage methods [3], [4]. On the other hand, power performances of MHs (hydrogen absorption and desorption rates) are strongly affected by the storage thermal management strategy, due to the highly exothermic/endothermic nature of hydrogenation/dehydrogenation reactions [5]. To improve thermal management efficiency, the

adoption of passive techniques is preferable, such as the coupling of MHs with Phase Change Materials (PCMs) [6], [7], [8], [9].

A crucial aspect in the design of MH-PCM storage tanks is the mutual influence of the MH and PCM materials deriving from their respective thermophysical properties at a given operating condition. Although an increasing number MH-PCM multidimensional modelling applications is emerging in the scientific literature [10], [11], [12], [13], [14], [15], [16], [17], [18], a lack of focus is clearly identifiable in the synthetic characterisation of the MH and PCM media in the context of the system's hydrogen storage/release performances.

The present paper represents a preliminary attempt to fill this gap, with an initial focus on the PCM characteristics and their impact on the hydrogen release rates from a cylindrical jacket-type MH-PCM tank. The remainder of the paper is organised as follows: in Section 2, the reference CFD model is introduced; in Section 3, results from a first batch of CFD tests are shown and briefly discussed; in Section 4, conclusions and perspectives for future work are drawn.

2. CFD modelling

The MH-PCM tank geometry and computational domain are shown in Fig. 1. The MH is a La-based AB_5 alloy, while an inorganic salt hydrate (*PCM₀*) has been selected as the baseline for the PCM properties sweep. This specific MH-PCM couple has already been found as optimal for close to
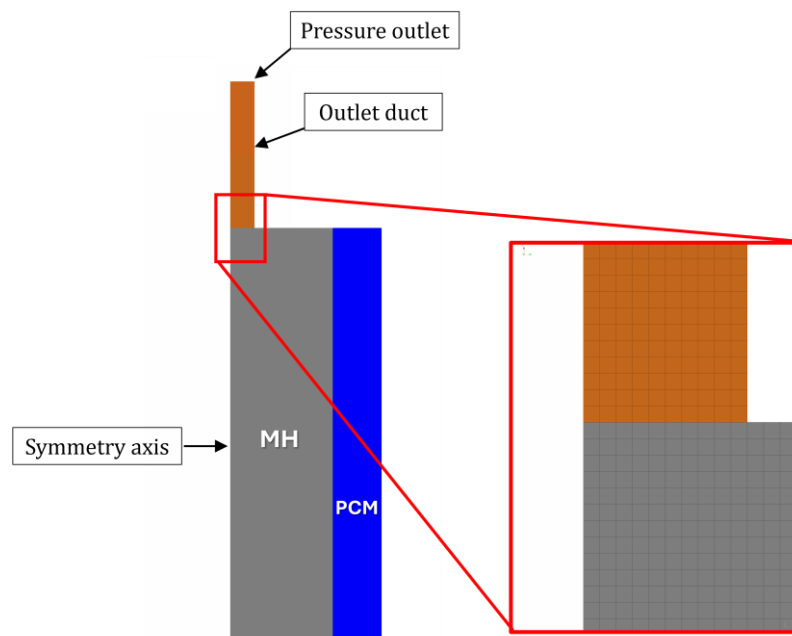
Figure 1. Schematics of the MH-PCM jacket configuration and computational mesh. The mesh is made by uniformly distributed quads with a 0.5 mm spacing.

atmospheric discharge pressures in previous publications [16], [18]. The most relevant MH and PCM properties are listed in Tables 1 and 2. As shown in Tab. 3, the reference geometry has a *H/D* ratio of 2 (*D = 2Ri*), while volumes have been optimised for the *PCM₀* medium at 1 atm discharge

pressure conditions in a previous work from the authors [18]. All CFD simulations are based on the following main assumptions:

a. the computational domain is 2D axisymmetric;
b. the external boundaries (except for the hydrogen outlet boundary) are all adiabatic walls
c. hydrogen is released from the MH alloy at a known and constant external pressure;
d. gaseous hydrogen is assumed to follow the ideal gas law;
e. the MH bed is considered as an isotropic porous medium;
g. local thermal equilibrium is assumed to hold within the AB_5-H2 system;
h. buoyancy is not considered for the heat transfer and melting phenomena within the PCM;
i. properties of the PCMs are considered constant and equal to the average between solid and liquid.

Table 1. Main properties of the AB_5-H_2 system.

Parameters	Description	Values
A_d	Plateau coefficient (desorption)	10.57
B_d	Plateau coefficient (desorption)	3704.6 K
C_d	Rate coefficient (desorption)	9.57 s^{-1}
$C_{p,g}$	Specific heat capacity (gas)	14890 J kg^{-1} K^{-1}
$C_{p,s}$	Specific heat capacity (solid)	419 J kg^{-1} K^{-1}
E_d	Activation energy (desorption)	16473 J mol^{-1}
ΔH_R	Enthalpy of reaction	30478 J mol^{-1}
k_b	Bed viscous resistance	10^8 m^{-2}
e	Bed porosity	0.5
λ_g	Thermal conductivity (gas)	0.1815 W m^{-1} K^{-1}
λ_s	Thermal conductivity (solid)	2 W m^{-1} K^{-1}
m_g	Dynamic viscosity (gas)	8.4 x 10^{-6} Pa s
ρ_{sat}	Saturated metal density	7259 kg m^{-3}
ρ_{emp}	H2-free metal density	7164 kg m^{-3}
$w_\%$	Gravimetric capacity (bed only)	1.32 %
m_{AB5}	Metal mass	~ 0.422 kg
m_{H2}	H2 storage capacity	5.6 g

Table 2. Main thermophysical properties of the PCM_0.

Parameters	Description	Values
$C_{p,PCM}$	Specific heat capacity	2250 J kg^{-1} K^{-1}
L_f	Latent heat of fusion	296000 J kg^{-1}
T_m	Melting temperature	303 K
λ_{PCM}	Thermal conductivity	0.95 W m^{-1} K^{-1}
m_{PCM}	Dynamic viscosity (liquid)	0.0042 Pa s
ρ_{PCM}	Density	1960 kg m^{-3}
α	Thermal diffusivity	$2.15 \cdot 10^{-7}$ m^2 s^{-1}
Pr	Prandtl number (liquid)	10

Table 3. Dimensional details of the MH-PCM tank.

Parameters	Description	Values
R_{H2}	H_2 outlet radius	0.5 cm
R_i	Internal radius	2.1 cm
R_e	External radius	3.2 cm
H	Height	8.5 cm
H/D	Slenderness	2
V_{MH}	MH volume (total)	118 cm³
V_{PCM}	PCM volume	154 cm³

The MH-PCM system model has been implemented in ANSYS® Fluent [19], [20], with the addition of ad-hoc developed User Defined Functions (UDFs) for dehydrogenation kinetics. In all the performed simulations, the numerical time step is set to 0.1 s, with a physical simulated time of 10^4 s. For further information on the modelling framework, see also [17], [18], [21].

3. Results & Discussion

Previous seminal works have already shown that, for a simplified PCM melting configuration (i. e. 2D with constant-temperature external forcing), a scaling relationship between the Nusselt, Rayleigh, Prandtl and Stefan numbers can be derived [22]. However, during hydrogen discharge heat is removed from the PCM and a conduction-dominant solidification process occurs, most likely driven by the Stefan number, thermal diffusivity and latent heat of the PCM [18].

All the tested configurations are shown in Table 4. Parameters with the *zero* subscript are representative of the baseline PCM properties reported in Tab. 2.

Table 4. Test PCM configurations for thermophysical parameters sensitivity.

Case	Thermal diffusivity	Latent heat	Prandtl number	Stefan number
Baseline	α_0	L_{f0}	Pr_0	Ste_0
Case 1a	α_0	$0.5L_{f0}$	Pr_0	Ste_0
Case 1b	α_0	$0.75L_{f0}$	Pr_0	Ste_0
Case 1c	α_0	$1.5L_{f0}$	Pr_0	Ste_0
Case 1d	α_0	$2L_{f0}$	Pr_0	Ste_0
Case 2a	$2\alpha_0$	$0.5L_{f0}$	$0.5Pr_0$	Ste_0
Case 2b	$1.33\alpha_0$	$0.75L_{f0}$	$0.75Pr_0$	Ste_0
Case 2c	$0.66\alpha_0$	$1.5L_{f0}$	$1.5Pr_0$	Ste_0
Case 2d	$0.5\alpha_0$	$2L_{f0}$	$2Pr_0$	Ste_0
Case 3a	α_0	L_{f0}	Pr_0	$0.5Ste_0$
Case 3b	α_0	L_{f0}	Pr_0	$0.75Ste_0$
Case 3c	α_0	L_{f0}	Pr_0	$1.5Ste_0$
Case 3d	α_0	L_{f0}	Pr_0	$2Ste_0$

For all configurations, the discharge pressure p_{out} is equal to 1.1 bar and the Stefan number is defined as follows:

$$Ste = \frac{c_{p,PCM}\left[T_m - T_{eq}(p_{out})\right]}{L_f},$$ (1)

with $T_{eq}(p_{out})$ being the metal hydride equilibrium temperature at the discharge pressure.
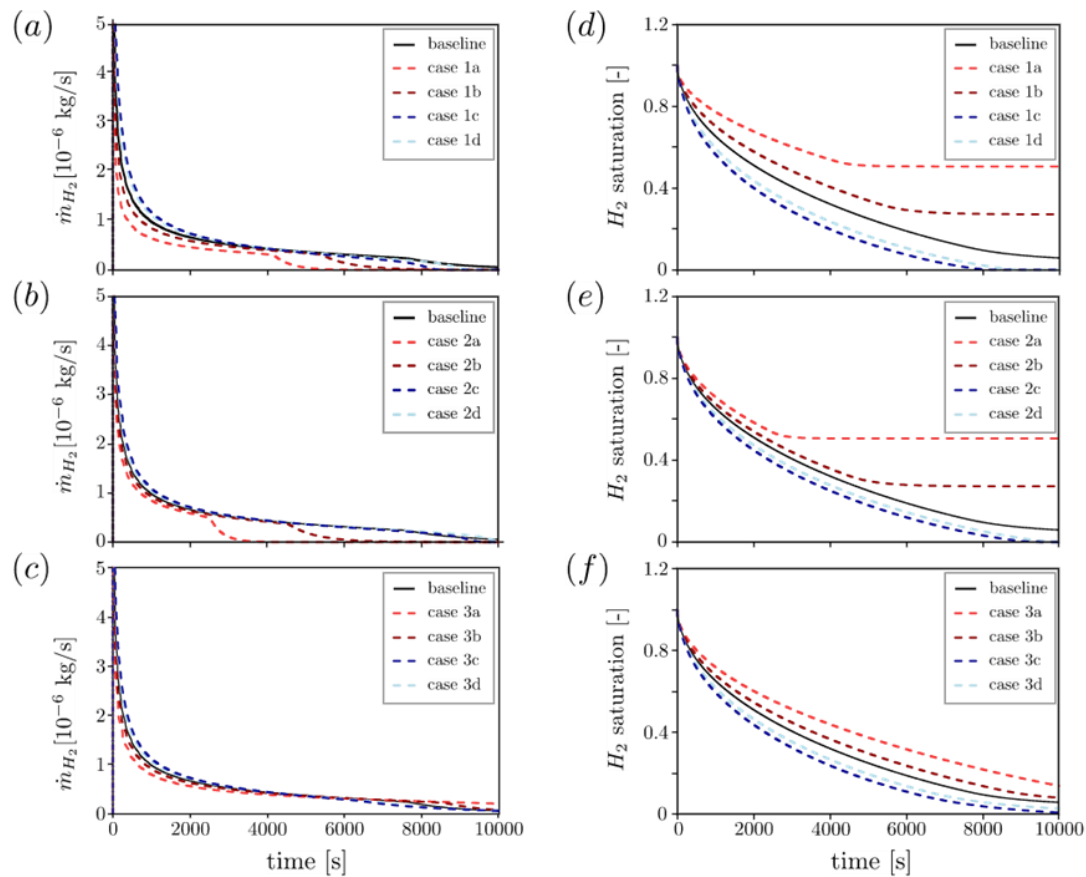

Figure 2. CFD test predictions. (a-c) Comparison between the baseline and perturbed configurations, in terms of delivered hydrogen mass flow vs. time. **(d-f)** Comparison between the baseline and perturbed configurations, in terms of hydrogen storage saturation level.

Results are shown in Fig. 2, in terms of instantaneous hydrogen mass flow and storage saturation level. The first two groups, displayed in Fig.2(a,d) and Fig.2(b,e), exhibit similar trends of both monitored quantities. In the first group the only variational parameter is the latent heat L_f, meaning that it is apparently the dominant one compared to the others included in Tab.4. Furthermore, Fig.2(b,e) suggest that, for sub-optimal L_f values (i. e. values that do not allow for complete hydrogen discharge due to the insufficient PCM latent heat capacity), a higher PCM thermal diffusivity is actually detrimental as it depletes faster the storage discharge capability.

Results from the third group show that, for a given L_f, increasing Ste produces marginal mass flow delivery improvements in the first part of the discharge transient.

4. Conclusions

In spite of the preliminary nature of the results shown above, the following concluding remarks can be drawn:

- in a coupled MH-PCM system, the latent heat L_f seems the primary sensitivity parameter on the PCM side;
- the impact of the PCM thermal diffusivity is closely related to the minimum L_f constraint: higher α values will generally increase the heat drain speed from the PCM, thus depleting faster its latent heat capacity;
- for given L_f and α values, the Ste influence on the hydrogen release dynamics is marginal and concentrated in the steeper part of the discharge curve.

Acknowledgements

References

[1] European Commission, "A hydrogen strategy for a climate-neutral Europe - COM(2020) 301 final," 2020. Accessed: Mar. 10, 2024. [Online]. Available: https://eur-lex.europa.eu/legal-content/EN/TXT/?uri=CELEX:52020DC0301

[2] Clean Hydrogen GB, "Clean Hydrogen JOINT UNDERTAKING (Clean Hydrogen JU) WORK PROGRAMME 2024," 2023.

[3] C. Drawer, J. Lange, and M. Kaltschmitt, "Metal hydrides for hydrogen storage – Identification and evaluation of stationary and transportation applications," *J Energy Storage*, vol. 77, Jan. 2024, doi: 10.1016/j.est.2023.109988.

[4] L. Pasquini *et al.*, "Magnesium- and intermetallic alloys-based hydrides for energy storage: Modelling, synthesis and properties," *Progress in Energy*, vol. 4, no. 3, Jul. 2022, doi: 10.1088/2516-1083/ac7190.

[5] H. Q. Nguyen and B. Shabani, "Review of metal hydride hydrogen storage thermal management for use in the fuel cell systems," *Int J Hydrogen Energy*, vol. 46, no. 62, pp. 31699–31726, Sep. 2021, doi: 10.1016/j.ijhydene.2021.07.057.

[6]   R. Sreeraj, A. K. Aadhithiyan, and S. Anbarasu, "Integration of thermal augmentation methods in hydride beds for metal hydride based hydrogen storage systems: Review and recommendation," *J Energy Storage*, vol. 52, Aug. 2022, doi: 10.1016/j.est.2022.105039.

[7]   V. K. Kukkapalli, S. Kim, and S. A. Thomas, "Thermal Management Techniques in Metal Hydrides for Hydrogen Storage Applications: A Review," *Energies (Basel)*, vol. 16, no. 8, Apr. 2023, doi: 10.3390/en16083444.

[8]   H. Q. Nguyen, M. Mourshed, B. Paul, and B. Shabani, "An experimental study of employing organic phase change material for thermal management of metal hydride hydrogen storage," *J Energy Storage*, vol. 55, Nov. 2022, doi: 10.1016/j.est.2022.105457.

[9]   S. Barberis, M. Rivarolo, and A. Sorce, "Thermal Energy Storage technologies for the optimal management of metal hydride hydrogen storage systems," in *Journal of Physics: Conference Series*, Institute of Physics, 2023. doi: 10.1088/1742-6596/2648/1/012061.

[10]   Y. Ye, J. Ding, W. Wang, and J. Yan, "The storage performance of metal hydride hydrogen storage tanks with reaction heat recovery by phase change materials," *Appl Energy*, vol. 299, Oct. 2021, doi: 10.1016/j.apenergy.2021.117255.

[11]   T. Alqahtani, S. Mellouli, A. Bamasag, F. Askri, and P. E. Phelan, "Thermal performance analysis of a metal hydride reactor encircled by a phase change material sandwich bed," *Int J Hydrogen Energy*, vol. 45, no. 43, pp. 23076–23092, Sep. 2020, doi: 10.1016/j.ijhydene.2020.06.126.

[12]   Y. Ye, J. Lu, J. Ding, W. Wang, and J. Yan, "Numerical simulation on the storage performance of a phase change materials based metal hydride hydrogen storage tank," *Appl Energy*, vol. 278, Nov. 2020, doi: 10.1016/j.apenergy.2020.115682.

[13]   F. Bouzgarrou, S. Mellouli, T. Alqahtani, and S. Algarni, "Parametric study of a metal hydride reactor with phase change materials and heat pipes," *Int J Energy Res*, vol. 46, no. 4, pp. 4588–4598, Mar. 2022, doi: 10.1002/er.7451.

[14]   A. Chibani, S. Merouani, N. Gherraf, I. Ferhoune, and Y. Benguerba, "Numerical investigation of heat and mass transfer during hydrogen desorption in a large-scale metal hydride reactor coupled to a phase change material with nano-oxide additives," *Int J Hydrogen Energy*, vol. 47, no. 32, pp. 14611–14627, Apr. 2022, doi: 10.1016/j.ijhydene.2022.02.171.

[15]   H. El Mghari, J. Huot, L. Tong, and J. Xiao, "Selection of phase change materials, metal foams and geometries for improving metal hydride performance," *Int J Hydrogen Energy*, vol. 45, no. 29, pp. 14922–14939, May 2020, doi: 10.1016/j.ijhydene.2020.03.226.

[16]   H. El Mghari, J. Huot, and J. Xiao, "Analysis of hydrogen storage performance of metal hydride reactor with phase change materials," *Int J Hydrogen Energy*, vol. 44, no. 54, pp. 28893–28908, Nov. 2019, doi: 10.1016/j.ijhydene.2019.09.090.

[17]   L. Bartolucci and V. K. Krastev, "On the Thermal Integration of Metal Hydrides with Phase Change Materials: Numerical Simulation Developments towards Advanced Designs," in *SAE Technical Papers*, SAE International, 2022. doi: 10.4271/2022-24-0018.

[18]   V. Krastev, G. Bella, G. Falcucci, L. Bartolucci, S. Cordiner, and V. Mulone, "Power Vs. Capacity Performances of Thermally Integrated MH-PCM Hydrogen Storage Solutions: Current Status and Development Perspectives," in *36th International Conference on Efficiency, Cost, Optimization, Simulation and Environmental Impact of Energy Systems, ECOS 2023*, Las Palmas de Gran Canaria, 2023, pp. 2183–2193. doi: 10.52202/069564-0197.

[19]   Ansys Inc., *ANSYS® Academic Research CFD, Release 2024 R1, Fluent User's Guide*. 2024. [Online]. Available: http://www.ansys.com

[20]   Ansys Inc., *ANSYS® Academic Research CFD, Release 2024 R1, Fluent Theory Guide*. 2024. [Online]. Available: http://www.ansys.com

[21]   V. K. Krastev and G. Falcucci, "Comparison of enthalpy-porosity and lattice Boltzmann-phase field techniques for the simulation of the heat transfer and melting processes in LHTES devices," *E3S Web of Conferences*, vol. 312, p. 01002, 2021, doi: 10.1051/e3sconf/202131201002.

[22]   P. Jany and A. Bejan, "Scaling theory of melting with natural convection in an enclosure," *Int. J. Heat Mass Transfer*, vol. 31, no. 6, pp. 1221–1235, 1988.